THE UPPER CRITICAL FIELD OF STOICHIOMETRIC AND OFF-STOICHIOMETRIC BULK, BINARY Nb_3Sn

M. C. Jewell, A. Godeke, P. J. Lee and D. C. Larbalestier

Applied Superconductivity Center, University of Wisconsin - Madison,
1500 Engineering Drive, Madison, WI 53706-1609, USA

ABSTRACT

Understanding the performance limits of Nb_3Sn superconducting wire is important to the design of superconducting magnets. Measuring these limits, however, is complicated by local chemical variations (on the scale of ~1 μm) in superconducting properties due to inhomogeneity in the wires. We have fabricated 1 mm^3, homogeneous, binary Nb_3Sn samples using hot isostatic pressing techniques on powder-in-tube bulk samples. The effects of Sn concentration and of Sn gradients on critical temperature (T_c) and the measured upper critical field ($\mu_0 H_{c2}$) were examined using high sensitivity magnetometry. $\mu_0 H_{c2}(0)$ varies linearly from 10.9 Tesla (T) at 19.3 at.% Sn to 31.4 T at 24.6 at.% Sn. The latter is an extraordinarily high value, suggesting that the Cu present in all practical Nb_3Sn conductors may actually suppress H_{c2}. Additionally, we demonstrate conclusively the propensity for stoichiometric Nb_3Sn to form below 1800°C, even when the nominal composition is decidedly off-stoichiometric. This shows the need for a fully volumetric measurement to accurately assess the effects of chemical inhomogeneity. Quantifying $\mu_0 H_{c2}$(%Sn) sheds light on the fundamental performance limits of Nb_3Sn and quantifies the material property loss due to the inhomogeneous nature of all commercial Nb_3Sn wires.

INTRODUCTION

Specifying the performance limits of Nb_3Sn is complicated due to the off-stoichiometric stability of the phase. The superconducting A15 phase is generally accepted to be stable within a solid solubility range extending from about 18 at.% to 26 at.% Sn [1]. T_c and $\mu_0 H_{c2}$ (and hence the critical current density, J_c) fall sharply with decreasing Sn content [2, 3]. Because of the brittle nature of the A15 structure, the conductor must be fabricated to final size from ductile components before creating the A15 material via heat treatment. The formation of the 3-5 μm Nb_3Sn filaments is hence a diffusion-controlled process, making the fabrication of a stoichiometric, homogeneous conductor difficult to achieve.

CP711, *Advances in Cryogenic Engineering: Transactions of the International Cryogenic Materials Conference - ICMC, Vol. 50,* edited by U. Balachandran

To overcome diffusional inhomogeneity, one may react the wire for longer times and at higher temperatures. The desire to support a high current density, however, requires a very high density of grain boundaries to pin the quantitized flux vortices of the superconducting state. Grain size increases with both reaction time and reaction temperature [4,5,6], so the fabrication of Nb_3Sn involves a fundamental compromise between the homogeneity of the material and the density of pinning centers available for maximizing vortex pinning. At present, in order to achieve the lowest feasible (~150 nm) grain size, it is accepted that the Nb – Sn reaction will not be driven to equilibrium, leaving a composition gradient in the A15 layer [7,8]. The effect of composition on J_c and the irreversibility field, H^*, has recently been modeled by Cooley *et al.* [9], and even small gradients have been shown to considerably reduce these primary superconducting properties. The quantitative dependence of $\mu_0 H_{c2}$ on Sn content is unclear, though a compilation of data from various sources (including the thin films of Orlando [10]) by Flükiger [3] suggests that $\mu_0 H_{c2}(0)$ peaks at 30.5 T at about 24.1 at.% Sn for binary Nb_3Sn. In this study we thus sought to measure $\mu_0 H_{c2}(T)$ for a broad composition range with a unified sample set.

EXPERIMENTAL PROCEDURE

The samples were fabricated using hot isostatic pressing (HIP) of a powder mix. This process was chosen to eliminate the inherent diffusion limitations of wire-based Nb_3Sn formation. Nb and Sn powders of <44 μm (–325 mesh; 99.9% and 99.8% metal basis, respectively) were mechanically mixed in various ratios from 18 at.% to 26 at.% Sn. The mixed powders were packed in Nb tubes with an inner diameter of 5.5 mm (0.216 in.), which were concentrically embedded in Cu tubes. The entire mixing and packing process occurred in an Ar glove box (99.9% Ar). The tubes were evacuated to $1x10^{-4}$ bar (80 mTorr) and then crimped to seal the billet. The HIP cycle consisted of 160 hours at 1020°C under $6.5x10^5$ bar (45,000 psi) of Ar gas (99.999% Ar). 1020°C was chosen to destabilize undesired Nb-Sn intermetallics ($NbSn_2$ and Nb_6Sn_5) [1], yet be below the melting point of Cu (1083°C).

A variety of post-HIP heat treatments were performed to homogenize the fully dense, two-phase material. Initially, a homogenization treatment of 166h/1250°C was performed on 10 mm-long cut-outs of the HIP tubes. These cut-outs were etched in a 1:1 HNO_3:H_2O solution to remove the Cu tube. This allowed for heat treating above the Cu melting point and ensured that Cu was not able to diffuse into the matrix material. The cut-outs were

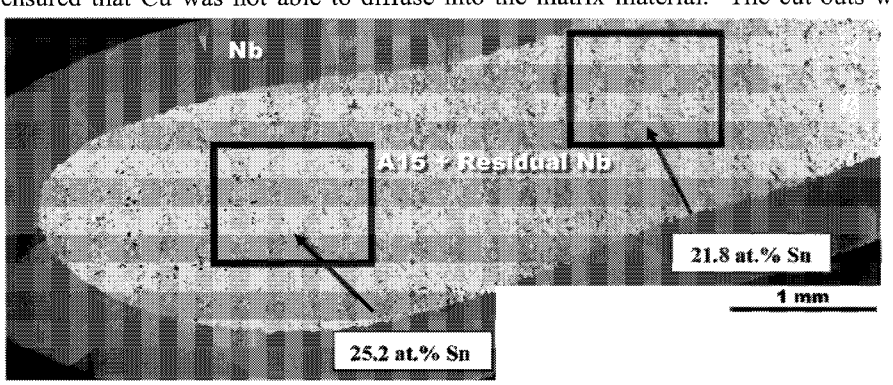

FIGURE 1. Long range Sn segregation in a nominally 24 at.% Sn HIP sample. A spatial separation of 3 mm showed a composition gradient (by EDS) of about 3 at.% Sn. The dark particles in the Nb_3Sn are residual Nb.

sealed in quartz tubes under a ~1x10^{-5} bar (10 mTorr) Ar atmosphere before heat treating. Metallographic examination after this step revealed the samples to be fully consolidated, but not fully homogenized. Additionally, long-range Sn segregation had occurred across the width of the samples during the HIP stage (see FIGURE 1). Further homogenization was performed at 24h/1800°C in a tungsten-mesh vacuum furnace. This step fully solutioned the residual Nb into the A15 phase. The afore-mentioned Sn segregation allowed us to section and subsequently characterize 1 mm^3 specimens of varying compositions from the same 6 mm HIP sample. In this manner multiple samples could be produced from one heat treatment specimen.

Magnetic characterization (T_c and $\mu_0 H_{c2}$) occurred in a Superconducting Quantum Interference Device (SQUID) in 0.005 T field and at 0.1 K temperature steps, and in a Vibrating Sample Magnetometer (VSM) in swept-field (0.6 T/min) mode. Sample homogeneity was characterized by specific heat (C_p) triangular approximation measurements (using the relaxation method) in a Quantum Design Physical Property Measurement System (QD PPMS) in zero magnetic field. $\mu_0 H_{c2}$ was defined as the first diamagnetic deviation of the signal from the paramagnetic background. The implications of this characterization method are examined in the discussion. Additionally, one bulk needle of 24.4 at.% Sn was characterized resistively in swept fields up to 30 T at the National High Magnetic Field Laboratory in Tallahassee, FL, and in swept fields up to 15 T at the Applied Superconductivity Center at the University of Wisconsin. Reference [11] gives additional experimental details on this resistive technique. The composition of the samples was checked by wavelength-dispersive spectroscopy (WDS) in a Cameca SX50 Electron Microprobe and by electron-dispersive spectroscopy (EDS) in a LEO 1550 field emission scanning electron microscope (FESEM).

RESULTS

Incompletely reacted samples

Early homogenization attempts involved a HIP-only thermomechanical treatment of 6.5x10^5 bar (45,000 psi) and 1020°C for 160h. Magnetic (VSM) $\mu_0 H_{c2}$ characterization after this step revealed both 18 at.% Sn and 24 at.% Sn samples to have identical upper critical field values (FIGURE 2), as determined by the magnetization slope change. This remarkable result was shown to be due to the presence of near-stoichiometric (high Sn)

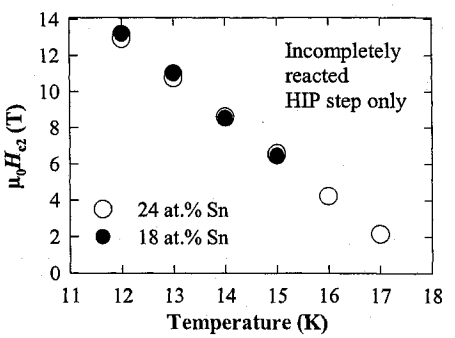

FIGURE 2. Initial $\mu_0 H_{c2}$ characterization of nominally 18 at.% Sn and 24 at.% Sn HIP samples, which were not fully homogenized (see FIGURE 1 for a representative microstructure). Both samples contained some high-Sn A15, resulting in identical upper critical fields as determined by magnetization slope change. This implies that either (1) the off-stoichiometric compound is not stable at 1250°C, or (2) the stoichiometric composition is kinetically favored as compared to the off-stoichiometric composition.

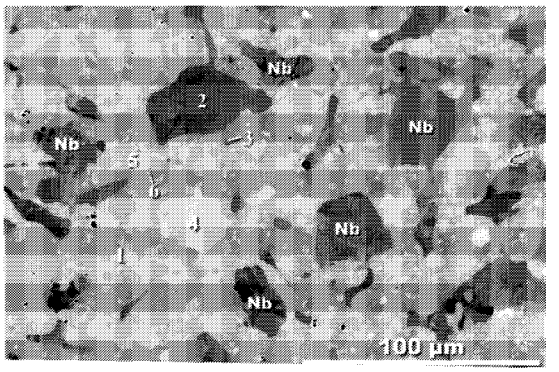

FIGURE 3. A positive correlation was seen between larger A15 grain size and higher Sn content in this nominally 18 at.% Sn sample. Note that the largest A15 grain (#4) has a Sn content of 26.2 at.%, while the finer grained material (#5) is decidedly off-stoichiometric.

Nb_3Sn grains in both samples, as revealed by electron dispersive spectroscopy (EDS) and FESEM. Thus the reaction appears to favor the nucleation of high Sn A15 over low Sn A15, even in a temperature regime where the accepted phase diagram predicts A15 stability down to 18 at.% Sn.

Further heat treatment of 166h/1250°C reduced the overall Nb volume fraction and succeeded in producing some off-stoichiometric Nb_3Sn (see FIGURE 3). At this stage, the largest grains were observed to be highest in Sn content, and the smallest grains (generally clustered around residual Nb islands) were observed to have the lowest Sn contents. Multiple subsequent heat treatments up to 166h/1350°C were not successful in homogenizing the off-stoichiometric samples.

Homogenized samples

It was not until a treatment of 24h/1800°C was applied that the off-stoichiometric samples became completely single-phase and homogeneous (this agrees well with observations by Devantay [2] and Vieland [12]). Due to transverse Sn segregation that occurred during the HIP step, we were able to extract four 1 mm^3 samples with varying Sn content from a single HIP specimen with an original composition of 22 at.% Sn. $\mu_0 H_{c2}(T)$ based on VSM measurements are presented in FIGURE 4 (next page). $\mu_0 H_{c2}(0)$ was observed to vary from 10.9 T at 19.3 at.% Sn to the exceptionally high value of 31.4 T at 24.6 at.% Sn. The curves are fitted with the Maki – de Gennes – Werthamer model (MGDW) [13,14,15,16,17], which has recently been shown by one of the authors [11,18] to very accurately fit resistive and magnetic $\mu_0 H(T)$ data from T_c to 1.4 K. To demonstrate the validity of this extrapolation, a bulk needle (8 mm x 1 mm^2) was extracted from a nominally 24 at.% Sn HIP sample and resistively measured in fields up to 30 T as described in [11].

The compositional information and superconducting properties of these samples are summarized in TABLE 1 (next page). The compositional variation data in TABLE 1 (column 3) were obtained by the specific heat measurement technique described earlier, and an example of such a C_p transition can be found in FIGURE 5. This technique was chosen to avoid magnetic shielding problems associated with magnetic measurements. The highest-Sn sample (24.7 at.% Sn) and the bulk needle (24.4 at.% Sn) compare well in homogeneity with the samples of Goldacker [19]. The composition (from T_c) column was obtained by extrapolating to T_c on FIGURE 4 and then converting to at.% Sn using the widely accepted T_c(%Sn) plot of Devantay *et al.* [2]. In general the T_c-derived

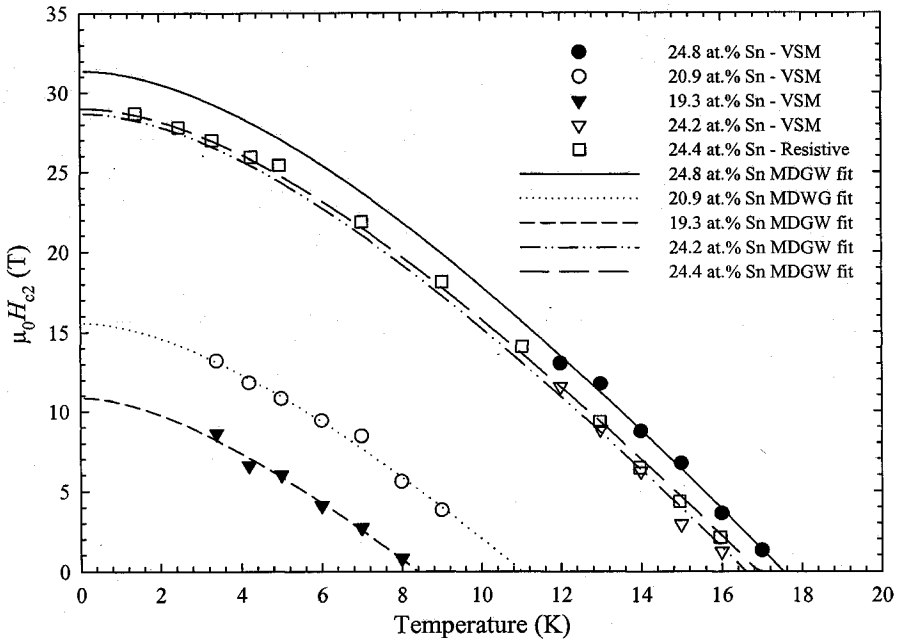

FIGURE 4. $\mu_0 H_{c2}$(T) for all four bulk samples measured in swept-field VSM plus one (24.4 at.% Sn) bulk needle measured resistively to 30 T. $\mu_0 H_{c2}(0)$ varies from 10.9 T for 19.3 at.% Sn to the surprisingly high value of 31.4 T for 24.8 at.% Sn.

compositions fall within the C_p-derived composition range, except for the bulk needle (T_c = 16.9 K). Here it is believed that the small cut-out from the needle used to ascertain the C_p transition width was not representative of the entire needle, but further sectioning of the needle was not desirable so as to retain sufficient sample length for future work. The WDS data are an average of random points along a line scan. Note that the WDS data agree well with the extrapolated T_c compositions and also with the C_p-deduced compositions except in the case of the 24.2 at.% Sn sample, where a local inhomogeneity near the line scan area likely depressed the Sn content.

TABLE 1. Compositional information and superconducting properties of magnetic and resistive samples.

T_c* K	**Composition (from T_c)*** at.% Sn	**Compositional variation⊗** at.% Sn	**$\mu_0 H_{c2}(0)$*** T	**Composition (from WDS)** at.% Sn
17.5	24.8	24.6 ± 0.2	31.4	24.2
16.9	*24.4*	*25.0 ± 0.1*	*29.0*	---
16.6	24.2	23.6 ± 0.7	28.7	21.8
11	20.9	20.2 ± 0.7	15.6	---
8.4	19.3	18.8 ± 0.6	10.9	19.2

Bulk needle (16.9 K T_c) characterized resistively

* From FIGURE 4.

⊗ From C_p transition width (see FIGURE 5).

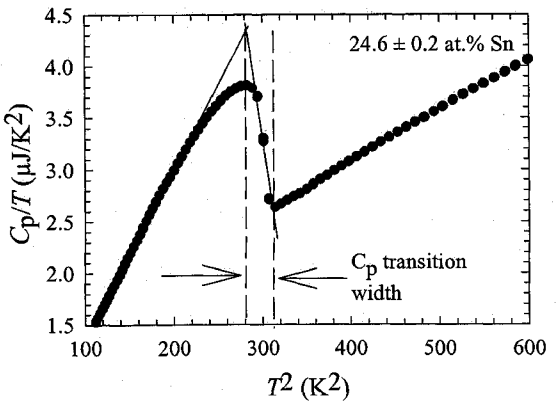

Figure 5. Specific heat superconducting transition width of a 24.6 at.% Sn sample, as determined by triangular approximation. This volumetric measurement allows for an accurate determination of the compositional inhomogeneity of the sample by relating the transition width (ΔT_c) to the corresponding composition distribution (Δ%Sn).

DISCUSSION

Implications of results

$\mu_0 H_{c2}$ is seen to vary linearly with Sn concentration, from 10.9 T at 19.3 at.% Sn to 31.4 T at 24.8 at.% Sn. FIGURE 6 shows our work compared with a compilation assembled by Flükiger [3]. Our data show a more linearized $\mu_0 H_{c2}$(%Sn), though we did not achieve a sufficiently Sn-rich sample to test the established result that $\mu_0 H_{c2}$ falls off sharply above 25 at.% Sn due to a cubic-to-tetragonal phase transition that occurs around 40 K [20]. FIGURE 6 represents, to our knowledge, the extent of the explicit $\mu_0 H_{c2}(0)$ as a function of Sn content available in the literature. Our maximum $\mu_0 H_{c2}(0)$ value of 31.4 T at 24.6 at.% Sn is extraordinarily high for binary Nb_3Sn and immediately raises the question of why such high values are not seen in "optimized" multifilamentary wires. While the small pre-strain exerted on wires by the stabilizing Cu may contribute to this depression, we believe such a large difference must be metallurgical in nature. We propose the possibility that interfilamentary Cu, which is present in all practical conductors (even

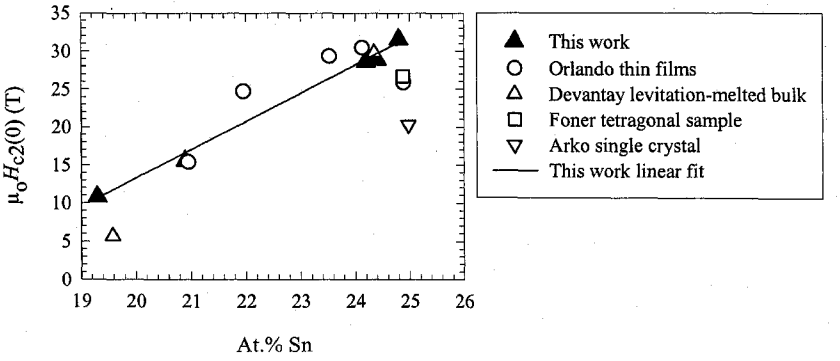

Figure 6. $\mu_0 H_{c2}(0)$ as a function of Sn composition for both this work and the available literature data. Note the generally linear dependence for our sample set and the surprisingly high value of 31.4 T at 24.8 at.% Sn.

so-called "binary" conductors that lack ternary additions such as Ta or Ti), may significantly suppress H_{c2}. Cu is necessary to catalyze the A15 formation reaction [21], which is in turn necessary to minimize grain growth and thus promote a high critical current, but may in fact have a negative chemical effect on the upper critical field. The role of Cu in Nb_3Sn formation and performance will be a key aspect of future work.

All practical superconducting wires are now accepted to have a bulk Sn gradient as an unavoidable consequence of the diffusional nature of the heat treatment. The times and temperatures required to drive the system to equilibrium are unacceptably long in terms of the corresponding grain growth. Cooley *et al.* [9] have recently shown, via a simple Sn-gradient model, the significant effect on H^* and J_c of such a Sn gradient (a 20% bulk pinning force depletion for even very flat gradients). Similar modeling focusing on H_{c2} may be enabled by our work, which quantifies the upper critical field loss associated with Sn depletion, to more accurately model superconductor strand behavior.

Composition distribution

The specific heat method of determining overall composition, combined with our data-fitting of the $\mu_0 H(T)$ curve, allows us to quantify the composition within the Sn gradient that is sampled by our magnetic and resistive measurement techniques. Convention holds that magnetic measurements such as VSM $\mu_0 H_{c2}$ and SQUID T_c probe the "best bit" of superconducting material, if the first deviation from normal state (paramagnetic) behavior is used as the transition criterion. Further, low-T_c superconducting compositions can be magnetically shielded by the higher-T_c compositions, depending on sample geometry. Similarly, resistive T_c measurements rely on the percolative nature of the current flow to seek the best bit of material. Such complications can thus give an inaccurate picture of the true composition gradients in the material. For this reason we use C_p, a truly bulk thermodynamic technique, to quantify the compositional variation in inhomogeneous material. These composition ranges (column 3 of TABLE 1), when compared to the "sampled composition" values determined from T_c (column 2 of TABLE 1) show that in all cases the true "best bit" of material is equal to or only slightly higher than the sampled composition by a marginal amount (the one exception being the bulk needle cut-out, the reason for which is discussed in the results). Thus this method of composition sampling allows us to extract useful superconducting properties even from imperfectly homogeneous samples.

An important, but not widely appreciated fact of Nb_3Sn diffusional formation is that in the presence of composition gradients, *some* volume of high-quality A15 will always form. The implication here is that vastly different samples (including wires) may have nearly identical upper critical field transitions when measured magnetically or resistively. This result is demonstrated vividly in FIGURE 2, where both an 18 at.% Sn and a 24 at.% Sn sample show identical $\mu_0 H_{c2}$ values. This propensity for high-Sn Nb_3Sn to form at practical reaction temperatures even when the overall Sn composition is decidedly off-stoichiometric should serve as a strong caution against using only magnetic or percolative resistive methods to quantify the primary superconducting properties of Nb_3Sn. Some high-Sn A15 will always form below 1800°C, and this "best bit" will dominate a magnetically-determined superconducting transition. The use of a fully volumetric technique (such as C_p or transport J_c) is needed to discern the full compositional distribution and its effect on material performance.

CONCLUSION

The upper critical field of Nb_3Sn was probed over a wide composition range using a single sample set and both magnetic (VSM) and resistive techniques. $\mu_0 H_{c2}(0)$ is shown to vary linearly from 10.9 T at 19.3 at.% Sn to 31.4 T at 24.6 at.% Sn. Homogenization of off-stoichiometric samples was unachievable below 1800°C, and magnetization $\mu_0 H_{c2}$ measurements showed conclusively that some high-Sn A15 is always formed in such inhomogeneous samples. Additionally, the compositional sampling method introduced here is shown to identify the Sn composition within the Sn gradient that dominates the magnetic characterization. Future work will focus on the role of Cu in solutionizing Nb into Nb_3Sn and the possible detrimental effect on $\mu_0 H_{c2}$.

ACKNOWLEDGMENTS

This work was supported by the US Dept. of Energy, Division of High Energy Physics (DE-FG02-91ER40643), and also benefited from NSF-MRSEC (DMR-9632427) supported facilities. The authors thank R. Lund and R. Sakidja for sample fabrication assistance, and L. D. Cooley for early sample characterization assistance and useful discussion. We gratefully acknowledge the assistance and expertise at the University of Wisconsin of W. L. Starch in metallographic preparation, A. A. Squitieri in physical properties measurements, and J. Fournelle in WDS characterization.

REFERENCES

1. Charlesworth, J.P., MacPhail, I. and Madsen, P.E., *J. Mat. Sci.* **5** (7), 580 (1970).
2. Devantay, H. *et al.*, *J. Mat. Sci.* **16**, 2145 (1981).
3. Flükiger, R., Schauer, W. and Goldacker, W., "Stress-Induced Instabilities in Nb_3Sn," *Superconductivity in d- and f-Band Metals*, edited by Buckel W. and Weber W., Karlsruhe, (1982).
4. Scanlan, R.M., Fietz, W.A. and Koch, E.F. *J. Appl. Phys.* **46** (5), 2244 (1975).
5. Livingston, J.D., *Phys. Stat. Sol. A* **44**, 295 (1977).
6. Bruzek, C.E. *et al.*, *IEEE Trans. Appl. Superconductivity.* **7** (2), 1041 (1997).
7. Hawes, C.D., Lee, P.J. and Larbalestier, D.C., "Measurement of the Critical Temperature Transition and Composition Gradient in Powder-In-Tube Nb_3Sn Composite Wires," *MT-16, IEEE Trans. Appl. Superconductivity* **10** (1), 988 (2000).
8. Smathers, D.B., *et al.*, "Scanning Auger Investigation of Commercial Multifilamentary Nb_3Sn Conductors," *IEEE Trans. Mag.* **Mag-19** (3), 1124 (1983).
9. Cooley, L.D. *et al.*, submitted to *J. of Appl. Physics*, 2003.
10. Orlando, T.P. *et al.*, *Phys. Rev. B* **19** (9), 4545 (1979).
11. Godeke, A. *et al.*, *Supercond. Sci. Technol.* **16** (9), 1 (2003).
12. Vieland, L.J., *RCA Review* **25**, 366 (1964).
13. de Gennes, P.G., *Phys. Condens. Matter* **3**, 79 (1964).
14. Maki, K., *Physics* **1**, 127 (1964).
15. de Gennes, P.G., *Superconductivity in Metals and Alloys*, Benjamin, New York, (1969).
16. Maki, K., in *Superconductivity*, Ed. R. Parks, Dekker, New York, (1969).
17. Helfand, E. and Werthamer, N.R., *Phys. Rev.* **147** (1), 288 (1966).
18. Godeke, A. *et al.*, in progress (2003).
19. Goldacker, W. *et al.*, *IEEE Trans. Appl. Superconductivity* **3** (1), 1322 (1993).
20. Mailfert, R. and Batterman, B.W., *Physics Letters* **24A** (6), 315 (1967).
21. LeFranc, G. and Müller, A., *J. Less-Common Metals* **45**, 339 (1976).